

ACCEPTED MANUSCRIPT

Fast optimized Monte Carlo phase-space generation and dose prediction for low energy X-ray intra-operative radiation therapy

To cite this article before publication: Marie Vidal *et al* 2019 *Phys. Med. Biol.* in press <https://doi.org/10.1088/1361-6560/ab03e7>

Manuscript version: Accepted Manuscript

Accepted Manuscript is “the version of the article accepted for publication including all changes made as a result of the peer review process, and which may also include the addition to the article by IOP Publishing of a header, an article ID, a cover sheet and/or an ‘Accepted Manuscript’ watermark, but excluding any other editing, typesetting or other changes made by IOP Publishing and/or its licensors”

This Accepted Manuscript is © 2018 Institute of Physics and Engineering in Medicine.

During the embargo period (the 12 month period from the publication of the Version of Record of this article), the Accepted Manuscript is fully protected by copyright and cannot be reused or reposted elsewhere.

As the Version of Record of this article is going to be / has been published on a subscription basis, this Accepted Manuscript is available for reuse under a CC BY-NC-ND 3.0 licence after the 12 month embargo period.

After the embargo period, everyone is permitted to use copy and redistribute this article for non-commercial purposes only, provided that they adhere to all the terms of the licence <https://creativecommons.org/licenses/by-nc-nd/3.0>

Although reasonable endeavours have been taken to obtain all necessary permissions from third parties to include their copyrighted content within this article, their full citation and copyright line may not be present in this Accepted Manuscript version. Before using any content from this article, please refer to the Version of Record on IOPscience once published for full citation and copyright details, as permissions will likely be required. All third party content is fully copyright protected, unless specifically stated otherwise in the figure caption in the Version of Record.

View the [article online](#) for updates and enhancements.

Fast optimized Monte Carlo phase-space generation and dose prediction for low energy X-ray intra-operative radiation therapy

M Vidal¹, P Ibáñez^{1,2*}, P Guerra^{3,4,5}, MF Valdivieso-Casique⁶, R Rodríguez⁶, C Illana⁶ and JM Udías^{1,2}

¹Grupo de Física Nuclear and IPARCOS, Dpto. Estructura de la Materia, Física Térmica y Electrónica, CEI Moncloa, Universidad Complutense de Madrid, Madrid, Spain

²Instituto de Investigación Sanitaria del Hospital Clínico San Carlos, Madrid, Spain

³Department of Electronic Engineering, ETSIT, CEI Moncloa, Universidad Politécnica de Madrid, Madrid, Spain

⁴Biomedical Research Center in Bioengineering, Biomaterials and Nanomedicine (CIBER-BBN), Spain

⁵MedLumics S.L, Tres Cantos, Madrid, Spain

⁶GMV, Tres Cantos, Madrid, Spain

E-mail: pbibanez@ucm.es

Abstract. Low energy X-ray Intra-Operative Radiation Therapy (IORT) is used mostly for breast cancer treatment with spherical applicators. X-ray IORT treatment delivered during surgery (ex: INTRABEAM®, Carl Zeiss) can benefit from accurate and fast dose prediction in a patient 3D volume. However, full Monte Carlo (MC) simulations are time-consuming and no commercial treatment planning system was available for this treatment delivery technique. Therefore, the aim of this work is to develop a dose computation tool based on MC phase space information, which computes fast and accurate dose distributions for spherical and needle INTRABEAM® applicators. First, a database of monoenergetic phase-space (PHSP) files and depth dose profiles (DDPs) in water for each applicator is generated at factory and stored for on-site use. During commissioning of a given INTRABEAM® unit, the proposed Fast and Optimized Phase-Space (FOPS) generation process creates a phase-space at the exit of the applicator considered, by fitting the energy spectrum of the source to a combination of the monoenergetic precomputed phase-spaces, by means of a genetic algorithm, with simple experimental data of depth dose profiles in water provided by the user. An in-house hybrid MC algorithm which takes into account condensed history simulations of photoelectric, Rayleigh and Compton interactions for X-rays up to 1 MeV computes the dose from the optimized phase-space file. The whole process has been validated against radiochromic films in water as well as reference MC simulations performed with penEasy in heterogeneous phantoms. From the pre-computed monoenergetic PHSP files and DDPs, building the PHSP file optimized to a particular depth-dose curve in water only takes a few minutes in a single core (i7@2.5 GHz), for all the applicators considered in this work, and this needs to be done only when the X-ray source is replaced. Once the phase-space file is ready, the hybrid Monte Carlo code is able to compute dose distributions within 10 minutes. For all the applicators, more than 95% of voxels from dose distributions computed with the FOPS+hybrid code agreed within 7%-0.5 mm with both reference MC simulations and measurements. The method proposed has been fully validated and it is now implemented into *radiance* (GMV SA, Spain), the first commercial IORT Treatment Planning System (TPS).

1. Introduction

Intra-Operative Radiation Therapy (IORT) is a modality of cancer treatment that combines the effort of surgery and radiation therapy in order to increment the rate of tumour control. In this treatment technique a high dose is administrated directly to the exposed tumour bed during surgery.

* The first two authors of this work have made equal contributions to the manuscript and the associated scientific research.

1
2
3
4 Mobile devices are increasingly used, such as dedicated electron accelerators or kilovoltage X-ray
5 devices.

6 The INTRABEAM® system (Carl Zeiss Surgical GmbH, Oberkochen, Germany) is a
7 commercial device dedicated to low energy X-ray IORT treatments. It is a mobile accelerator that
8 includes a miniature electron-beam driven X-ray source (Dinsmore *et al.* 1996, Beatty *et al.* 1996)
9 and allows treating various localizations with different applicators (Sethi *et al.* 2018).

10 Low-energy X-ray IORT is a subject of debate and there has been some controversy
11 regarding the potential benefits of the technique. Although longer-term follow up randomized trials
12 would be needed to definitely settle this issue, the 5-year TARGIT-A (Vaidya *et al.* 2014) trial
13 showed promising clinical results for breast cancer irradiation. Indeed X-ray IORT exhibited similar
14 local control and less toxicity, especially chronic skin toxicity (Sperk *et al.* 2012) in comparison to
15 patients treated with external beam radiotherapy. IORT is also used as a boost for breast cancer
16 treatments, since intra-operative treatments present some potential advantages to the patient, such as
17 avoiding the delay between surgical resection and treatment, minimizing the risk of geographic
18 misses associated with external beam boost techniques (Kraus-Tiefenbacher *et al.* 2005), or
19 incrementing patient comfort when compared to other boost methods (Sedlmayer *et al.* 2017).
20 However, there are some obstacles that difficult the task of finding evidence of therapeutic benefit
21 of this technique. Dose prescription is not personalized, the actual dose distribution delivered is
22 unknown, and the calculation tool provided by vendors is based on water profiles (Clausen *et al.*
23 2012).
24

25 Previous studies have already pointed out the impact of not considering heterogeneities in
26 dose calculation for low energy X-ray IORT. The use of water instead of CT-derived densities may
27 lead to inaccurate dose calculations, particularly in regions where variable tissue densities and
28 heterogeneities may be present (Bouزيد *et al.* 2015). Deviations from dose prescription have been
29 found of up to 34% in the case of breast irradiation (Hensley 2017) and larger than 300% for bone
30 tissues (Chiavassa *et al.* 2015). Some of these uncertainties in tissue assignment, target assessment
31 and applicator placement could be reduced by means of treatment planning systems. However,
32 hitherto there was no commercial treatment planning tool which allows accurate and fast
33 determination of the dose received during an irradiation using X-ray IORT.

34 There are several previous studies aiming to characterize the INTRABEAM® device.
35 Detailed Monte Carlo simulations of a miniature 50 keV accelerator used to treat brain tumours
36 were performed by Yanch and Harte with ITS 3.0 (Yanch and Harte 1996). More specifically,
37 Bouزيد *et al.* developed a Geant4/GATE code suitable to INTRABEAM® treatment issues (Bouزيد
38 *et al.* 2015) while Ebert and Carruthers used EGSnrc to model the INTRABEAM® source (Ebert
39 and Carruthers 2003). High accuracy is reached with full Monte Carlo (MC) simulations, however it
40 is still a time-consuming technique and it is not suitable for real-time planning in the Operating
41 Room (OR). The use of phase-space (PHSP) files reduces the overall computation time. Therefore,
42 in order to speed up dose calculation, Clausen *et al.* developed a Geant4-based source model using
43 PHSP files which decreased computation time to 12 minutes for a full gynecological treatment
44 (Clausen *et al.* 2012). However, that technique was suitable only for water dose calculations and
45 simulation time would increase when applied to more complex geometries with heterogeneities.
46 Moreover, standard PHSP files lack flexibility in manipulating data, exhibit huge storage
47 requirement, and need resources for reading-in the stored data during simulation (Chetty *et al.* 2007,
48 Schach von Wittenau *et al.* 1999). Alternatively, Nwankwo *et al.* obtained PHSP from a virtual
49 source model to generate photons for a specific INTRABEAM® source defined in Geant4
50 (Nwankwo *et al.* 2013). A reasonable calculation uncertainty was achieved within 2 hours of
51 simulation. However, dose computation time is still too long for OR irradiations or to be
52 implemented in commercial treatment planning systems (TPS).
53

54 Indeed, in order to develop an accurate dose computation tool, the main problem we face is to
55 obtain a description of the radiation produced by a particular X-ray INTRABEAM® device. A
56 detailed MC simulation of each device and X-ray source is just too complicated to be of any
57 practical use in the clinical routine. The aim of this work is to develop a fast and accurate dose
58 calculation tool which can obtain the radiation produced by any given INTRABEAM® applicator,
59 tuned to the user's device from simple experimental data, and which is suitable for a fast and easy
60

deployment as a treatment planning system. In order to achieve this goal, we propose an optimization method that uses a pre-stored database of monochromatic PHSP files and depth dose profiles (DDP) which can be tuned to reproduce every user's device, just knowing the experimental DDP in water for the given device. This development is supplemented with a hybrid Monte Carlo dose calculation algorithm to allow fast and accurate computation of dose distributions, taking into account the source parameters as well as complex patient data (heterogeneities, CT data). Dose computed by this process was compared to dose obtained by realistic MC simulations of the sources, for spherical and needle applicators, and to experimental data in water.

2. Materials and methods

2.1. INTRABEAM® device and spherical treatment applicators

The INTRABEAM® system consists of an electron gun which emits electrons that are accelerated to a maximum of 50 kV by the accelerating unit. Two pairs of bending coils guide the electron beam through the probe to the gold target, where bremsstrahlung photons are generated. This results in an approximately isotropic dose distribution (Eaton 2012, Schneider *et al.* 2009) around the X-ray Source (XRS). The probe may be encapsulated with different applicators, which shape the dose distribution. In particular, a simple needle applicator can be added in the case of stereotactic radiosurgery for brain tumours (Douglas *et al.* 1996) or spinal metastases irradiation (Schneider *et al.* 2011, Wenz *et al.* 2010). Spherical applicators are mostly employed for breast cancer (Vaidya *et al.* 2010), but its use is being extended to other treatments such as glioblastomas (Giordano *et al.* 2014).

2.2. Dose calculation with the Hybrid Monte Carlo algorithm

A fast and precise dose calculation algorithm was developed in order to compute dose in voxelized volumes. The hybrid MC dose calculation algorithm takes into consideration photoelectric, Rayleigh and Compton interactions. Particles are sampled at the surface of the applicator following the stratified approach described by Guerra *et al.* (Guerra *et al.* 2014), using the information stored in the phase-space, and transported throughout the volume in steps of length dr , whose value is typically smaller than half the voxel size. At each transport step, the probability P for each interaction type is computed as $P=1-\exp(-\mu \cdot dr)$, with μ being the attenuation coefficient coming from either photoelectric, Rayleigh or Compton effects extracted from PENELOPE-2008 database (Salvat *et al.* 2008). If an incident photon undergoes photoelectric interaction with a probability P_{PE} , the photon transfers all its energy E_{ph} to the electron, and it is assumed that it is immediately absorbed at the voxel where the photoelectric interaction occurred. If a photon undergoes Compton interaction with a probability P_C , the photon is scattered and part of its energy is transferred to the recoil electron, which we also assume that it is absorbed in the voxel where the Compton interaction occurred. Finally, if a photon undergoes Rayleigh interaction, the photon is scattered and no energy loss takes place. Rayleigh and Compton scattering angles have been precomputed and stored for the different materials in a compact form. These approximations are fair for the energies considered here, for biological materials (lung, muscle, bone), if voxel sizes of the order of 0.25 mm^3 or larger are employed.

In order to reduce variance, the following aspects are included in the simulation (Ibáñez 2017a,b):

- Meta-histories (m-histories) approximation. Every primary particle (m-history) represents the fate of many photons. This m-history can scatter or undergo photoelectric effect, with a given probability. After interacting, m-histories are not removed, but instead their weights are updated after each spatial time progression. Energy deposition in the voxel is computed from the change of weight of the m-history.
- Condensed and forced interactions. After each simulation step, the fraction of the primary m-history that interacts is computed, its weight removed from the weight of the primary m-history. Secondary particles (due to Compton or Rayleigh) are generated with their corresponding weights.

- A fluence normalization is implemented to reduce dose artifacts due to poor statistics or suboptimal sampling of the region of interest, allowing dose distributions free from statistical noise from a low number of initial meta-histories.

2.3. Fast Optimized Phase-Space-based (FOPS) Dose Computation process

The dose optimization and calculation method proposed in this work has been separated in three phases. Firstly, a database of monoenergetic PHSP files and DDPs in water was computed from detailed simulations at the external surface of the INTRABEAM® applicators. These PHSP files were parameterized for easier handling and storage. Secondly, a PHSP file tuned for each device is obtained by a linear combination of all the monoenergetic sources. To this end, an experimental DDP provided by the manufacturer is fit to a linear combination of DDPs from the monoenergetic sources (Iaccarino *et al.* 2011). The fit is performed by means of a genetic algorithm (Fernandez-Ramirez *et al.* 2008) and the resulting optimized PHSP file reproduces the user's data. Finally, dose is calculated from this optimized PHSP file with the Hybrid Monte Carlo code we have developed (Ibáñez 2017a,b, Vidal *et al.* 2014a,b). A scheme of the FOPS+Hybrid MC process is shown in figure 1. We describe these phases below:

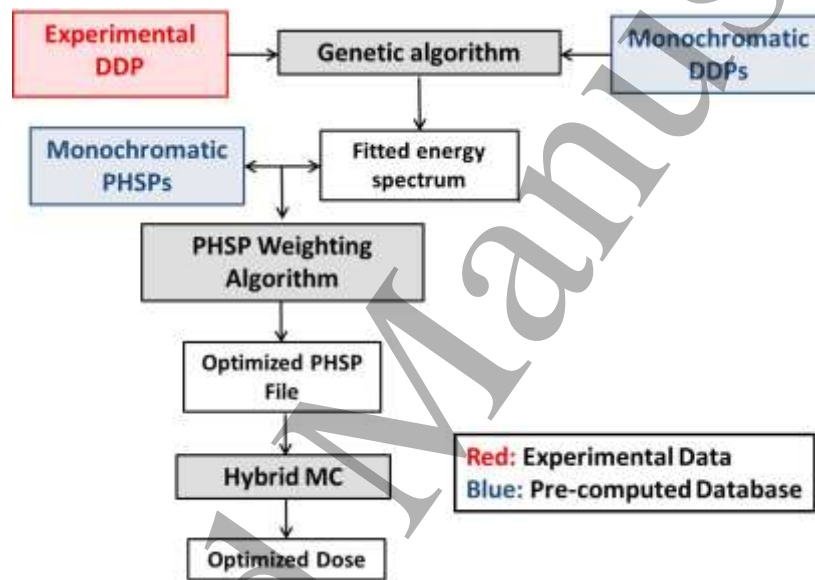


Figure 1. Scheme of the FOPS computation process

2.3.1. Database generation. This step needs to be done once for each applicator upstream the dose calculation process. First of all, a set of MC simulations performed to obtain a database of monoenergetic PHSP was run with penEasy (Sempau *et al.* 2011), a main program designed for PENELOPE-2008 (Baro *et al.* 1995, Salvat *et al.* 2008). This MC package is easy to use, very accurate, and it has been extensively benchmarked (Ma and Jiang 1999, Sempau *et al.* 2003, Ye *et al.* 2004, Chica *et al.* 2009). With penEasy we simulated a quasi-punctual source of photons emitting isotropically from the center of the applicators and interacting with a standard geometry per each applicator size. 50 MC simulations, from 1 keV to 50 keV, were performed with 10^8 initial particles for each applicator. The resulting monoenergetic PHSP files were collected at the external surface of the applicator and stored in IAEA format (Capote *et al.* 2006), i.e. represented by n -tuples which include particle type, energy, (x,y,z) position, angles of emission (u_x, u_y, u_z) and weight of each particle. Afterwards, the PHSP files previously stored were used to compute the corresponding monoenergetic DDPs in water with the fast hybrid Monte Carlo dose calculation algorithm described before. This database is independent on the actual energy spectrum of any given X-ray source. The database generation is time-consuming, but it needs to be performed only once.

2.3.2. *PHSP parameterization.* Since standard PHSP files can be heavy to use, in this work they are parameterized and redundant variables are removed, taking advantage of the symmetry of the spherical applicators. The method was based on a similar approach used to parameterize PHSP files generated for IORT dose calculation with electrons (Herranz *et al.* 2015) and to reduce the size of the PHSP. It also reduces statistical noise from a given number of simulated histories in the computation of the PHSP.

Owing to the geometry of the needle and spherical applicators, a PHSP history can be fully defined by its Energy (E) and two angles α and β , one to position the particle in the surface of the sphere, and another to determine the direction of emission of the particle with respect to the direction of the radius of the sphere at the point of emission.

The definition of the angles is presented in figure 2. We allow for a dependence for the fluence of the particles on their forward or backward position along the surface of the sphere, i.e., on the angle α . We assumed azimuthal symmetry around the axis of the applicator, and azimuthal symmetry of the direction of emission of the particles with respect to the direction of the radius of the sphere at the point of emission of the particle. To compute the actual dose, the condensed information contained in this compact PHSP needs to be “debinned” to produce histories supplementing the information in the PSHP with two azimuthal angles randomly picked in the range from 0° to 360° . One of them, combined with α , fixes the location of the emission point for the particle in the surface of the sphere. The second one, combined with β , determines the direction of emission of the particle.

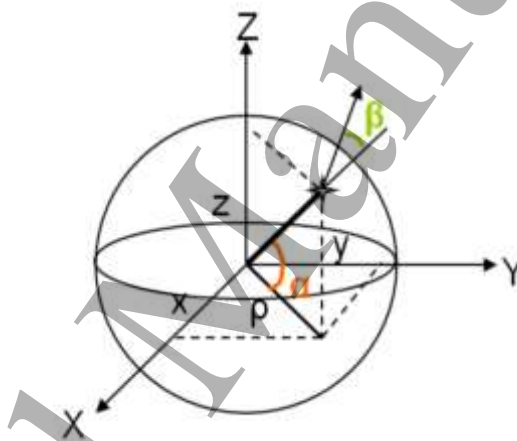


Figure 2. Angles α and β used to parameterize PHSP files.

Regarding bin size, a trade-off between accuracy of the representation and number of bins was made. Starting from a reference PHSP with 100 million particles, it was binned in successively coarser bins in the variables previously described. The dose produced by the PHSP from coarser bins, once debinned, was compared to the one of the unbinned PHSP. With the bin sizes employed in this work, the doses from binned and unbinned PHSP agree well within the 1%-1 mm gamma criteria (Low *et al.* 1998) (more than 99% of the voxels passed the test). The PHSP files have been finally parameterized with 50 bins in energy, ranging from 0 to 50 keV, 200 bins in α , from 0° to 180° , and 200 bins in β , ranging from 0° to 20° .

2.3.3. *Optimization of the energy spectrum.* For each applicator, the vendor provides only the DDPs in water, measured in-house. The method we propose is able to optimize the energy spectrum of the PHSP at the external surface of each applicator using this experimental data. This fitting step should be carried out each time the experimental curve changes, from one applicator to another, from one X-ray source to another, etc. In the first phase of the PHSP optimization process, the monoenergetic DDPs are going to be adjusted to the experimental dose by means of a genetic algorithm (Fernández-Ramírez *et al.* 2008). The genetic algorithm will generate an optimized energy spectrum which weights the relative contributions of the monochromatic DDPs that reproduces the experimental dose data. The energy spectrum was defined as a simple mathematical

function describing the bremsstrahlung behavior of the energy spectrum and the characteristic rays of 50 keV X-rays impinging in gold and other materials of the target. Equation (1) describes the bremsstrahlung background of the energy spectrum $S_{background}(E)$ without taking into account characteristic lines (Kramers 1923)

$$S_{background}(E) = (E - E_1)^a \cdot \left(\frac{E_0}{E} - 1 \right)^b \quad (1)$$

where E_0 is the maximum energy of the 50 keV photon beam energy spectrum and E_1 the cut-off energy. a and b are a filtration parameter and Kramers' law adjustment parameter, respectively.

Further, as shown in equation (2), some characteristic X-ray lines from gold were added to the background, at energies 9.5, 12 and 13.5 keV, as measured by Schneider *et al.* at the surface of the probe (Schneider *et al.* 2010) and further confirmed by our own detailed Monte Carlo simulations of the X-ray source (Ibáñez, 2017a).

$$S_{spectrum}(E) = S_{background}(E) + c(E) \cdot I_p(E) \quad (2)$$

Where $I_p(E)$ is the intensity of the characteristic line at energy E relative to the other two lines, and $c(E)$ is the mixing parameter determining the amplitude of the characteristic lines relative to the spectrum background intensity.

The DDP is adjusted from a weighted sum of the 50 monoenergetic DDPs previously computed in water. Thus the resulting fitting function is just the energy spectrum of the actual source. For each experimental DDP provided by the user, the parameters E_1 , E_0 , a , b and c are varied and results in a specific energy spectrum shape (with different bremsstrahlung backgrounds and characteristic line intensities) reproducing each experimental DDP.

Once the energy spectrum is optimized, the monoenergetic PHSP files are weighted by the corresponding energy spectrum for each applicator, obtaining an optimized PHSP tuned to the experimental data. A scale factor is computed in order to scale the final dose to the experimental data. From these scale factors and the optimized PHSP, absolute dose distributions are obtained from the hybrid MC algorithm described above.

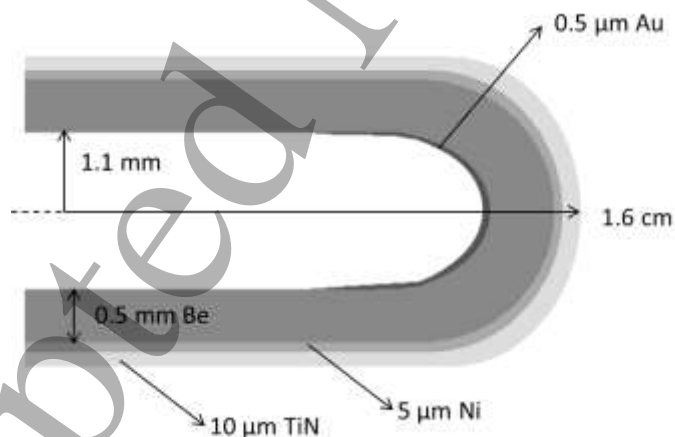


Figure 3. Schematic view of the INTRABEAM® XRS used for the energy spectrum characterization.

2.4. Monte Carlo characterization of the X-ray source.

A detailed characterization of the XRS has been performed with penEasy (Sempau *et al.* 2011) in order to determine the shape of the energy spectrum and to generate reference dose distributions to compare against the FOPS+hybrid MC process. The geometry of the XRS has been accurately described in the literature (Dinsmore *et al.* 1996, Beatty *et al.* 1996, Yanch and Harte 1996). We defined the geometry as a 1.6 cm length beryllium needle with 1.1 mm inner radius and thickness of 0.5 mm with a 0.5 μm layer of gold at the end of the probe. The beryllium needle is surrounded by a first layer of nickel with a thickness of 5 μm and a second layer of TiN with a thickness of 10 μm

(see figure 3). Regarding the electron source impinging on the gold target, it was characterized with a Gaussian energy distribution with a mean energy of 50 keV and a full width at half maximum (FWHM) of 5 keV. The electron beam does not impact in the entire target surface, but in an annular area between 0.6 and 0.8 mm radii (Clausen *et al.* 2012). The dose was scored at the exit of the probe surface with $4 \cdot 10^{10}$ initial particles in order to accumulate more than 200 million particles in the scoring plane, obtaining a statistical uncertainty of the simulation to around 2%. No variance reduction techniques were used. The voxel size employed in the simulation was 0.25 mm. This simulation was split up into 200 simulations running in parallel for around 12 hours each in a cluster based on an 8 core Intel® Xeon® CPU @ 2.00 GHz.

2.5. Validation of the Fast Optimized Phase-Space generation and Hybrid MC dose computation for needle and spherical applicators

First of all, PHSP were generated and optimized to reference data for spherical and needle applicators. Then, dose distributions were computed with the hybrid MC algorithm in various phantoms. Dose distributions obtained with the FOPS-hybrid were compared to measurements, when they were available, and to dose distributions computed by standard reference PenEasy MC simulations. 2D and 3D gamma evaluations were performed to check the accuracy of the results. The steep gradient of INTRABEAM® dose distributions was taken into account when selecting distance-to-agreement and dose difference criteria (Eaton and Duck 2010, Chiavassa *et al.* 2015). Since most points will fail on distance and not on dose, 7%-0.5 mm asymmetric tolerances were selected. We considered that a given solution would pass the gamma evaluation if at least 95% of the points with dose equal or higher than 5% of the maximum dose had gamma values smaller than one (Herranz *et al.* 2015).

2.5.1. Water measurements. On the one hand, dose distributions from the FOPS+hybrid process were compared to experimental 2D dose maps in water provided by Zeiss Medical (Oberkochen, Germany) for all applicators. A water-equivalent phantom, specifically designed to measure 2D dose distributions along the applicator axis, was employed. It consists of two blocks made of solid water with an applicator-shaped hole. The film is located between the two blocks and the applicator is placed in the phantom hole. Dose distributions were measured with EBT3 Gafchromic films and scanned using an Epson Expression 10000XL (US Epson, Long Beach, CA) flatbed scanner at least 24 hour post-irradiation. A scanning protocol described by Avanzo *et al.* (Avanzo *et al.*, 2012) was adopted. Film images were analyzed using an in-house image manipulation routine written with MATLAB 7.6.0.324 (MathWorks, Natick, MA, USA) based on the three channel technique (Micke *et al.* 2011).

Reference DDPs were extracted from the films along the applicator axis and used to fit the monoenergetic PHSP files and DDPs by means of our optimization algorithm. Optimized PHSP files were generated and then used to compute dose with the Hybrid Monte Carlo. 10^7 histories were simulated with the Hybrid MC in $401 \times 401 \times 401$ voxels phantoms, with $0.25 \times 0.25 \times 0.25$ mm³ voxel size.

Dose was compared to verify the accuracy of the fitting process in the whole 2D dose map. The first 0.5 millimeters of film next to the surface of the applicator were removed from the comparison to avoid artifacts in the experimental dose distribution caused by the deformation that the border of the films experience when cut to adapt to the applicator surface.

2.5.2. Heterogeneous phantoms. The FOPS+hybrid MC process was tested against penEasy simulations in heterogeneous phantoms representing possible clinical situations for all applicators. In the first situation, the applicator was surrounded by a layer of water 5 mm thick, and then bone, representing a glioblastoma treatment or a partial breast irradiation close to a rib. The second situation represented the applicator surrounded by a layer of bone 1.5 mm thick, and then lung, to simulate a Kypho-IORT treatment. And the third phantom represents the applicator surrounded by water and then lung also representing a breast irradiation.

On the one hand, reference dose distributions were calculated with penEasy using the energy spectrum derived from the XRS characterization. Full MC simulations were performed for the three situations with $2 \cdot 10^9$ histories, without variance reduction techniques. On the other hand, FOPS+hybrid process was used to predict dose distributions in the same phantoms. Doses were first calculated in water with penEasy and their DDPs were used as the input in the FOPS optimization process. Then, the optimized PHSP files were used to calculate dose distributions with the hybrid MC in the three heterogeneous phantoms with 10^7 m-histories. Both calculations were performed with a voxel size of $0.25 \times 0.25 \times 0.25$ mm³. 3D gamma evaluations were performed with 7%-0.5 mm tolerances.

2.5.3. Clinical cases. Two clinical situations were also included in the validation of the FOPS+hybrid MC. The first one is the case of a partial breast irradiation with a 3 cm diameter spherical applicator, while the second one is a Kypho-IORT treatment of the spine. For both clinical cases, 3D CT scans of the patients were used to compute dose distributions with penEasy and with the FOPS process combined with the Hybrid MC. The same number of histories and voxels sizes as for the heterogeneous phantoms were taken. 3D gamma evaluations were performed with 7%-0.5 mm tolerances to compare both calculations.

3. Results

3.1. Detailed Monte Carlo simulations

For the x-ray source, we have compared the energy spectrum obtained with the full MC simulation and the experimental energy spectrum (Schneider *et al.* 2010), shown in figure 4. The agreement is good, except for the characteristic peaks at the lower end of the spectrum, which are more visible in the simulation than in the measurements. However, for these very small energies the experiment just may not be sensitive enough, and in any case they have little relevance in the dose computation.

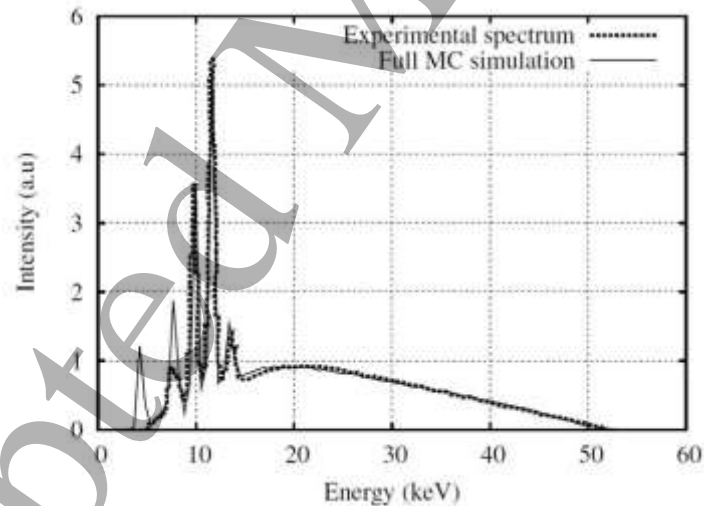


Figure 4. Energy spectra at the surface of the XRS obtained experimentally and with the full MC simulation.

3.2. Energy spectrum optimization

For each applicator, the genetic algorithm developed in this work fits the depth dose distribution to the experimental DDP provided by the user *via* an optimized energy spectrum. Figure 5a shows an example of a fitted energy spectrum compared to the experiment (Schneider *et al.* 2010) for the 35 mm diameter spherical applicator. It shows that the energy spectrum obtained with the genetic algorithm is following the same trend than the experimental spectrum through the characteristics rays and general shape. The energy spectra obtained for the other spherical applicators are very similar to the energy spectrum shown for the 35 mm diameter spherical applicator. The fitting of the depth dose distributions is shown in figure 5(b), where the experimental profiles (dots) and

fitted depth dose curves (solid lines) times the square of the distance to the surface of the applicators for all the applicators is compared.

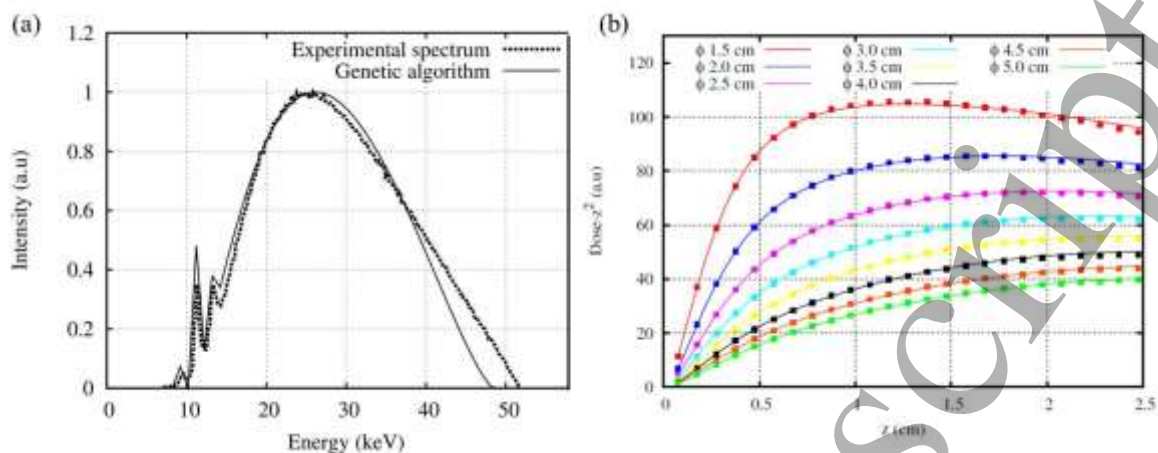


Figure 5 (a) Comparison of energy spectra obtained experimentally and the one resulting from the fit to the experimental DDP with the genetic algorithm for the 35 mm diameter spherical applicator. (b) Experimental DDP (dots) and fitted DDP (solid lines) times the square of the distance to the surface of the applicator for the different applicators.

3.3. Validation of the FOPS dose computation process for needle and spherical applicators

3.3.1. Comparison against experimental measurements in water. Figure 6 shows an example of 2D dose distributions in water for a 45 mm diameter applicator obtained with the FOPS+hybrid process from the reconstructed PHSP file and measured with a radiochromic film, the corresponding 2D gamma map and a comparison of dose profiles along the indicated directions, as well as the corresponding dose differences. Direction p1 was chosen to evaluate the dose differences in the area where anisotropy is more present, in contrast to direction p2 that has been selected in a more isotropic region. Both p1 and p2 dose profiles have been compared with a dose profile extracted from the isotropic dose map obtained from the hybrid MC. Dose differences are below 5% in most of the area, but increase up to about 15% in the backward direction next to the applicator, as it can be seen in figure 6d. The gamma evaluation distribution was performed for 7%-0.5 mm criteria with a 5% threshold and normalized to the maximum dose. Table 1 summarizes the gamma results for all spherical applicators. Almost all the cases have more than 95% voxels fulfilling the criteria. The main differences between experimental and simulated images are present in the backward direction, and are due to the anisotropy of the real XRS, which is not taken into account in the FOPS computation. Results are still reasonably good despite the fact that an isotropic particle emission of the source is assumed in the FOPS process.

Table 1. 7%-0.5 mm gamma evaluation (5% threshold) between radiochromic films and FOPS+hybrid MC in water for spherical applicators.

Applicator diameter (ϕ)	15 mm	20 mm	25 mm	30 mm	35 mm	40 mm	45 mm	50 mm
Water phantom (%)	96.2	98.1	98.1	97.9	96.9	94.2	97.6	94.2

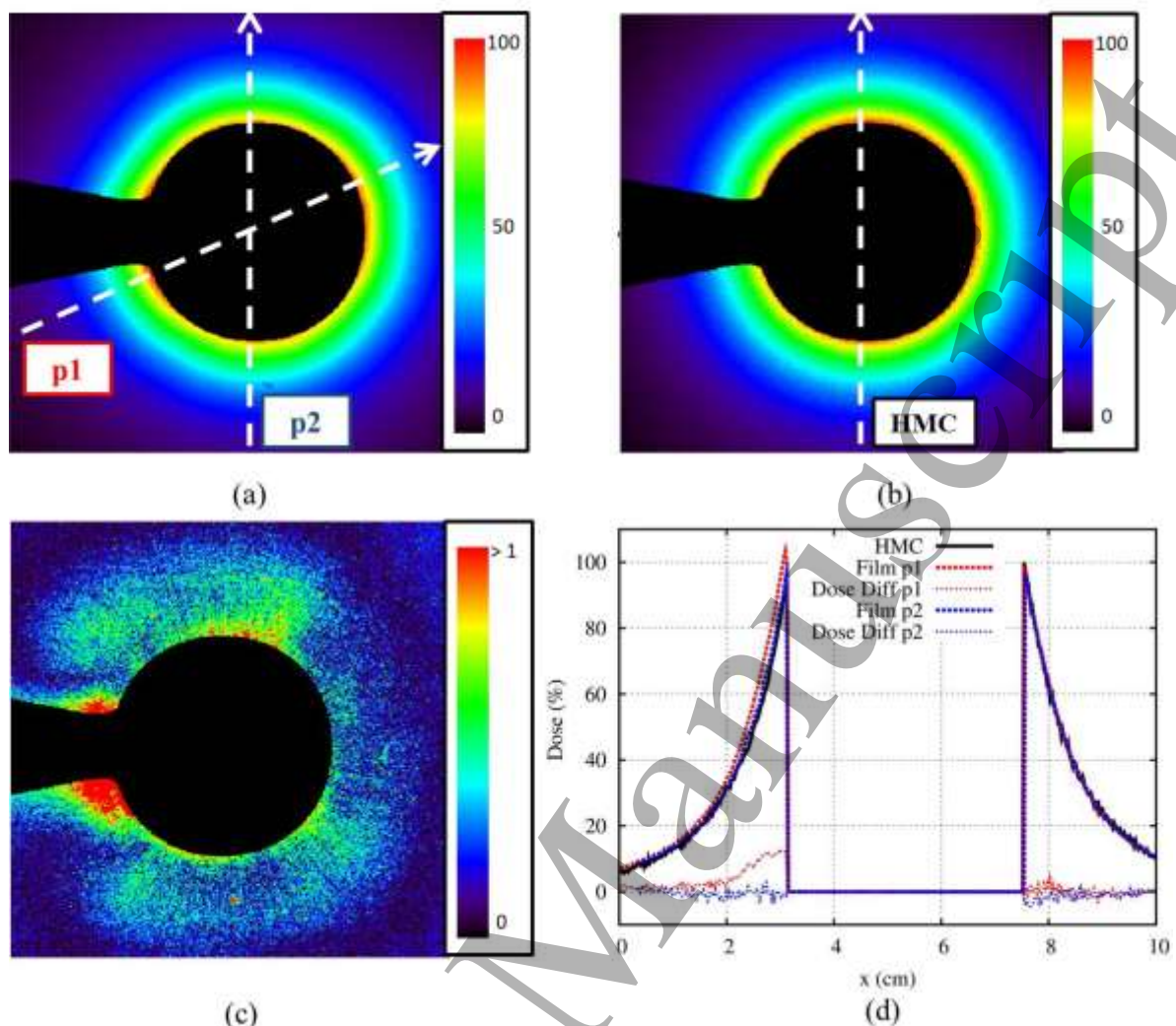


Figure 6. 2D dose distributions in water for a 45 mm diameter spherical applicator obtained from (a) radiochromic films, (b) FOPS dose computation process + hybrid MC (HMC) (c) 7%-0.5 mm Gamma distribution and (d) dose profiles along the indicated directions p1 and p2, and the corresponding dose differences. Dose agreement is very good, except in the areas close to the applicator neck, due to the isotropy assumption in the computed dose.

3.3.2. Comparison against MC simulations in heterogeneous phantoms. 3D dose distributions were computed with both Monte Carlo simulations (penEasy) and FOPS+hybrid MC in the heterogeneous phantoms described previously in section 2.5.2 for all applicators (including needle). In figure 7 a comparison of transverse views and the corresponding gamma evaluation is presented for the 30 mm diameter spherical applicator in the water/bone phantom. The differences between both dose distributions come from the convention of assigning dose to voxels in penEasy and in the FOPS algorithm. A 3D gamma index comparison with 7%-0.5 mm criteria between both dose computations is summarized in Table 2, for the 3 different phantoms and all the applicators. The results are similar from one phantom to another, as dose computation quality does not depend on the considered materials. It can be seen that FOPS+hybrid dose predictions and full MC simulations are in good agreement (7%-0.5 mm 3D gamma index passing rate is 97.8 %).

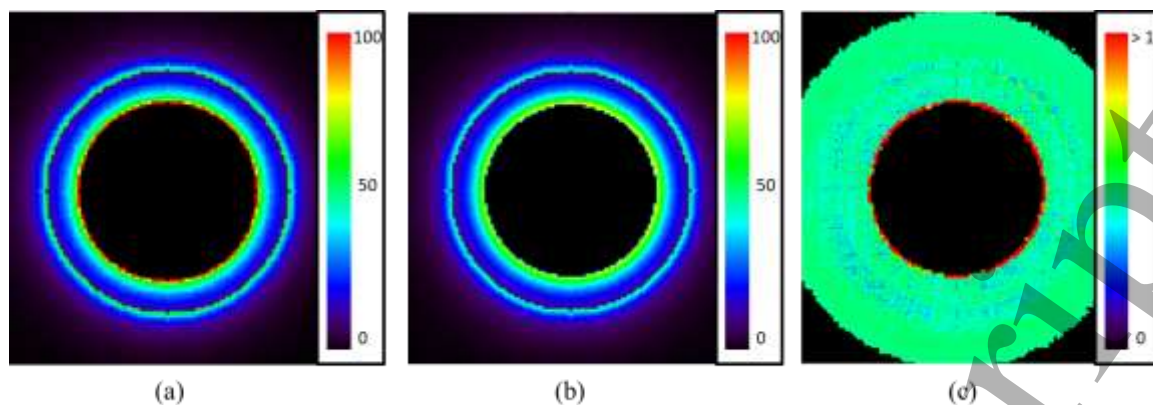


Figure 7. Transverse view of 3D dose distributions delivered by the 3 cm diameter applicator in the water/bone phantom, computed with penEasy (a), and with the Hybrid Monte Carlo from the FOPS process (b), and the 7%-0.5 mm gamma evaluation (c).

Table 2. Results of the 7%-0.5 mm (5% threshold) gamma index comparison between full MC simulations and FOPS+ hybrid MC dose computation in heterogeneous phantoms for needle and spherical applicators.

Applicator type	Needle	ϕ 15 mm	ϕ 20 mm	ϕ 25 mm	ϕ 30 mm	ϕ 35 mm	ϕ 40 mm	ϕ 45 mm	ϕ 50 mm
Water/bone (%)	96.0	97.7	97.7	97.8	97.8	97.8	97.5	97.4	96.6
Bone/Lung (%)	98.9	99.0	99.1	98.9	97.4	96.1	96.8	96.6	95.7
Water/ lung (%)	96.2	98.8	98.9	99.0	99.1	99.1	99.1	99.0	97.6

3.3.3. Comparison of MC simulations in clinical cases. Figure 8 shows the comparison of the two considered clinical situations, where dose maps computed from penEasy and the hybrid MC from the FOPS process are compared for a partial breast irradiation and a Kypho-IORT case. A 3D evaluation in terms of gamma index has been performed with 7%-0.5 mm criteria and 5% threshold and it is also represented. 98.2% of the voxels passed the criteria for the partial breast irradiation dose calculation and 95.2% of the voxels passed the criteria for the Kypho-IORT dose calculation. Slight differences can be observed at the surface of the applicator in both cases and this is due again to the different convention of assigning dose to voxels in penEasy and in the hybrid MC algorithm, but in general, the FOPS+hybrid MC process provides very accurate dose computation in patient data.

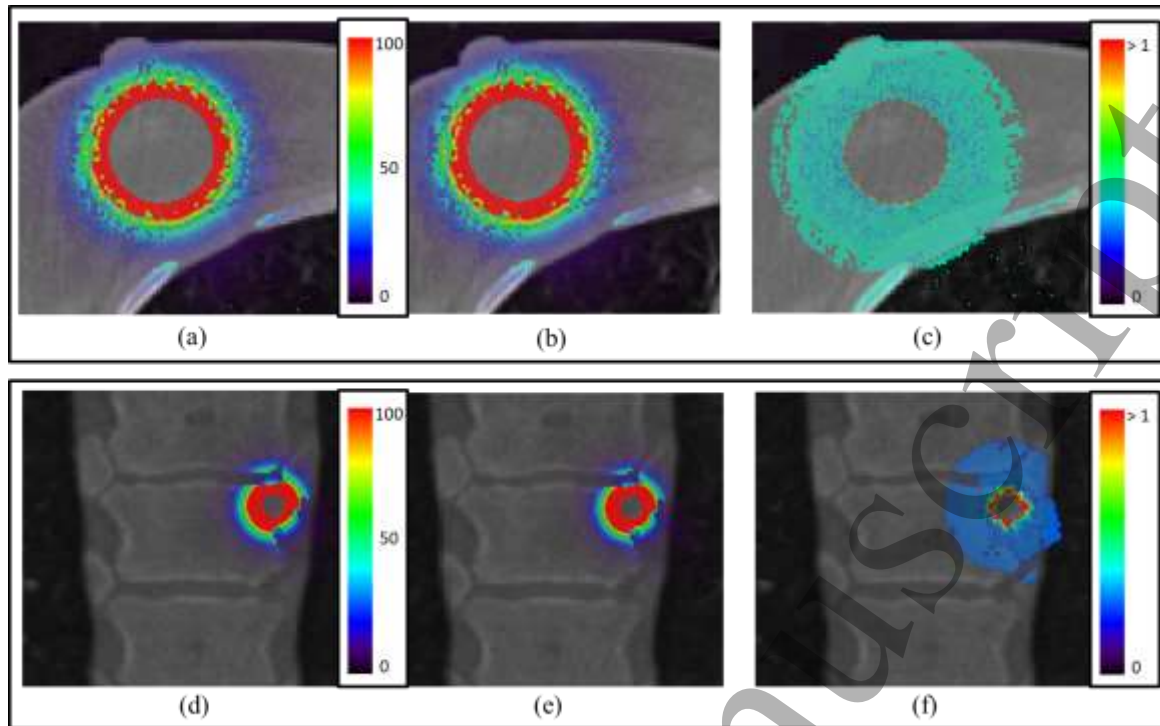


Figure 8. Dose maps from penEasy (a) and the hybrid MC from the FOPS process (b), and the gamma evaluation (c) delivered by the 30 mm diameter applicator in the partial breast irradiation simulation. Dose maps from penEasy (d) and the hybrid MC from the FOPS process (e), and the gamma evaluation (f) in the Kypho-IORT calculation with the needle applicator.

4. Discussion

In this work we have described a dosimetric tool capable of providing a realistic dose distribution for INTRABEAM® spherical and needle applicators. First, we have developed a fast tuning tool to generate PHSP files optimized to any user's device, providing as input only an experimental DDP in water (see figure 1). Second, we have developed a dose calculation algorithm suitable for INTRABEAM® working energies that includes the accuracy of a MC algorithm and calculates dose distributions in a fraction of the time. The combination of both developments allows the user to obtain accurate doses from an optimized PHSP file tuned to a particular device within minutes.

The dose computational tool described in this work has been validated against reference data that included experimental measurements and Monte Carlo simulations. A detailed simulation of the INTRABEAM® X-ray source was performed in order to obtain a realistic X-ray spectrum to use in the rest of the MC simulations. The simulated energy spectrum of the XRS was compared to an experimental measurement (figure 4). The calculated energy spectrum is very similar to the experiment and shows resemblance to previous studies (Nwankwo *et al.* 2013, Yanch and Harte 1996), although some differences can be seen in the characteristic X-ray peaks, mostly at low energies, where the lowest energy peak (4.41 keV), corresponding to Ti characteristic X-rays is only seen in the simulation, and the second peak (7.54 keV), matching the Ni transitions, presents a higher intensity in the simulation than in the experiment. However, the most intense peaks, corresponding to the Au lines (9.54, 11.53 and 13.24 keV), exhibit essentially the same intensity as the experiment. Observable differences in the lowest energy peaks can be either due to the limited efficiency of the detector for X-rays of such small energy, or by a slight difference in the thickness of the biocompatible layer employed in the simulation with respect to the actual material. Nevertheless, these differences bear little relevance for actual dose estimations, as such low energetic X-rays are absorbed within the first micrometers of the applicator.

The optimization algorithms developed in this work to tune PHSP to experimental data perform accurately. Some fitting results are shown in figure 5. DDPs for all applicators are very well reproduced and the fitted energy spectrum of the 35 mm diameter spherical applicator

resembles the measured spectrum. The parameterization employed to compress the PHSP reduces the number of lines of PHSP files to a maximum of 2 million, making the problem amenable to our algorithms and the PHSP files easier to handle.

The FOPS+hybrid MC process was tested against experimental measurements in water and against MC simulations in heterogeneous phantoms and clinical patient data. 2D and 3D gamma computations were used to evaluate the results. Dose difference and distance-to-agreement values of 7% and 0.5 mm respectively were chosen to take into account the high dose gradients in the INTRABEAM® dose distributions (Eaton and Duck 2010). As for distance-to-agreement requirements of the TPS for IORT, a 0.5 mm in the areas of steep gradients should be deemed more than good enough. For these kind of treatments, patient/applicator positioning, and co-registration with the CT or other image employed to compute dose, 1 mm accuracy in distances is either in the state of the art or within reach in the immediate future, thus we should demand the TPS to exceed this accuracy, and this is so if it fulfills a 0.5 mm criteria. On the other hand, if the IORT procedure is unable of obtaining distance control for patient-applicator positioning better than 1 mm, there is no point in further increasing the TPS accuracy. Distance-to-agreement of 0.5 mm certainly saturates the accuracy that can be obtained with IORT procedures in the near future.

For the water validation against experimental measurements, Gafchromic EBT3 films were used. There has been some controversy regarding the use of radiochromic films for low energy X-rays. EBT, as well as EBT2, showed energy dependence in the kilo-voltage energy range (Ebert *et al.* 2003, Sutherland and Rogers 2010), which made these dosimeters not suitable for low-energies. However, EBT3 have been found to be a more suitable dosimeter for INTRABEAM®'s working energies (Brown *et al.* 2012, Hill *et al.* 2014), and they can be used for absolute and relative dosimetry, measuring of output factors and beam profiles (Steenbeke *et al.* 2016). DDPs were extracted from the films and used to fit the monochromatic DDPs and PHSP files. Dose distributions obtained from the tuned PHSP files were then compared to the complete 2D dose maps measured with the films. We observed that the main differences between measurements and the Hybrid MC calculation were due to the anisotropy present in the backward direction of the actual applicators, as seen in the radiochromic films (figure 6a). The approach we considered for our spherical dose definition considers isotropy in the particle emission, and therefore, does not reproduce the experimental excess of dose close to the neck of the applicator. This can be seen in figure 6d, where dose profiles along two directions have been selected, one through the area where the experimental anisotropy is more significant (profile p1), and the other in a region far from the neck of the applicator (profile p2). Dose differences up to 14% are observed in the neck region, while for the remainder applicator measured and simulated dose differences are well below 5%. This anisotropy can result in an increment of the dose delivered of up to 3 Gy next to the applicator neck for a standard breast treatment, where dose prescription is usually 20 Gy at the surface. However, the volume presenting the anisotropy is restricted to a small region in the vicinity of the applicator neck, an area where very often no tissue is located, and anyway far enough from critical structures such as lung, heart or the rib cage. A 7%-0.5 mm gamma test with a 5% threshold resulted in more than 95% of voxels passing for most cases. For two applicators the level of fulfillment of the gamma criterion was marginally inferior. These two cases corresponded to measurements where the films were centered poorly and dose maps were incomplete, thus only a small area could be evaluated. Overall, there is reasonable agreement of simulations and experiment, considering the uncertainty associated with film dosimetry (Sorriaux *et al.* 2013) and possible experimental setup errors. The error of the system used (film, scanner and procedure) was approximately 2% for voxels with more than 5% of the maximum dose.

Further improvement to the FOPS+hybrid MC process would be achieved by introducing an angular-dependent function in the fluence of the X-ray beam, thus the anisotropy of the spherical applicators would be reproduced. Anisotropy can be fully addressed in the procedure proposed. However, backward/forward anisotropy in INTRABEAM® spherical applicators is not part of the manufacturer commissioning workflow, nor it is routinely measured, as it is considered a minor correction. Therefore, despite the technical feasibility of introducing anisotropy in the fitting process, the lack of experimental data does not allow us to consider it in the PHSP optimization.

1
2
3
4 A further validation of the FOPS+hybrid MC process was done when comparing with
5 heterogeneous phantoms. PHSP file derived from DDPs in water were used to predict dose in
6 different heterogeneous phantoms resembling clinical situations, as well as in two clinical cases.
7 Good results were obtained in general, with a 7%-0.5 mm gamma evaluation yielding a 98%
8 average pass rate (5% threshold). The uncertainty of a MC simulation is inversely proportional to
9 the square number of initial histories, more exactly, to the square number of energy depositing
10 interaction in each voxel. We are dealing with 10^9 - 10^{10} histories in every reference simulation, thus
11 statistical noise at the voxels with 5% of dose or more is below 1%.

12 Absolute dose can also be reproduced with our algorithm. A scale factor that adjusts our
13 algorithm to absolute dose is recovered from the comparison with the reference MC and the
14 experimental DDP. The formalism includes this scale factor that is going to be applied to the final
15 dose so that it is scaled to the input experimental DDP. This way, if the experimental DDP input in
16 the procedure is a relative dose, with 100% at the maximum dose in water, we will obtain as well a
17 relative dose distribution with a maximum value compared to maximum value in water. But if the
18 initial DDP used to input in the algorithm is an absolute dose, the optimized PHSP file will generate
19 absolute dose distributions.

20 Computation time of the FOPS fitting process (genetic + PHSP weighting algorithms) varies
21 on each case. The genetic algorithm is the most time consuming procedure. The number of dose
22 values of the experimental profile and the voxel size employed in the simulation of the
23 monochromatic DDPs are a contributing factor in the running time of the code. It goes from less
24 than one minute up to 6-7 minutes running in one core of an Intel® Xeon® CPU @ 2.00 GHz. The
25 PHSP weighting algorithm is faster. In this part of the procedure, the computation time is highly
26 dependent on the number of bins in which each PHSP file has been discretized. The computation
27 time of this part of the fitting process takes about 40 seconds for the spherical applicators. In all
28 cases the overall time needed to generate an optimized PHSP file that reproduces a given
29 experimental DDP is below 10 minutes, and this optimization only needs to be done once for each
30 X-ray source deployed. Once the PHSP is fine-tuned, dose calculation with the Hybrid MC requires
31 around 10^7 histories to achieve 2% statistical noise, which takes less than 10 minutes of simulation
32 time in one core of an Intel® Xeon® CPU @ 2.00 GHz, while $2 \cdot 10^9$ histories were needed in
33 penEasy, equivalent to several days of computation time in the same computer.

34 The need of dose planning systems for INTRABEAM® has been already discussed in the
35 literature (Hensley 2017, Hill *et al.* 2014). Previous studies trying to develop a treatment planning
36 system for the INTRABEAM® proved this to be a very challenging goal mostly due to computation
37 time issues. Dose calculation must be very fast because it should be possible to repeat the
38 calculations once the patient situation right after surgery is known, and it should be even possible to
39 compute the dose under different scenarios (energy, applicator size or angle, different shielding) so
40 that oncologists and medical physicists can tune the setup within minutes, in order not to delay the
41 procedure and to finish the surgical intervention as fast as possible. Clausen *et al.* developed a
42 Monte Carlo model to calculate dose for a cylindrical INTRABEAM® applicator within 12 minutes
43 in water (Clausen *et al.* 2012). However, the approximation they described is not suitable for
44 heterogeneous media and if a full simulation is needed, the required calculation time would increase
45 up to 5 h (Nwankwo *et al.* 2013). A virtual model of the INTRABEAM® source was also
46 developed by Nwankwo *et al.* (2013) generating a source model tuned to each device as in the
47 FOPS process. However, dose calculation required 2 hours, which is too long to be used for dose
48 treatment planning in the OR during an IORT treatment.

49 Alternatively, the FOPS+hybrid process described in this work can be used for treatment
50 planning, as it combines a fast tuning tool to generate PHSP files optimized to any user's device
51 with a dose calculation that exhibits the accuracy of a MC method while obtaining dose
52 distributions in a fraction of the time. The combination of both tools allows the user to obtain a dose
53 distribution from a PHSP tuned to reproduce his device within minutes. The presented work is valid
54 not only for needle and spherical applicators but also for other INTRABEAM® applicators such as
55 flat and surface. Future studies will be focused on extending the process to include other applicators
56 and performing a complete validation of the codes against experimental measurements.
57
58
59
60

5. Conclusion

As far as the authors know, previous to this work there was no readily available TPS for the INTRABEAM® device (Hensley 2017). The aim of this work was to develop a dose computation tool based on MC phase space information to rapidly and accurately compute the dose in a first approach for spherical applicators. The hybrid MC algorithm and the phase-space generation tool described here have been fully validated against full MC simulations and experimental data, in homogeneous and heterogeneous phantoms, as well as in clinical 3D patient data. These tools have been integrated into *radiance* (GMV, Tres Cantos, Spain), a planning software for intra-operative radiation therapy (Valdivieso-Casique *et al.* 2015, Pascau *et al.* 2012), thus extending the number of supported devices within this tool. With this software, the user is able to use commissioning measurements to calibrate the treatment device, estimate dose distributions in complex scenarios with the aid of advanced techniques (Schneider *et al.* 2017) and finally perform dose-volume histogram (DVH) calculations and procedure reporting.

Acknowledgements

This work is supported by the Comunidad de Madrid (S2013/MIT TOPUS-CM, PRONTO-CM), Spanish Ministry of Science and Innovation (FPA2010-17142), Spanish government (XIORT grant IPT-2012-0431-300000, ENTEPRASE PSE-300000-2009-5, PRECISION IPT-300000-2010-3 and FPA2015), by European Regional Funds, by CDTI under the CENIT program (AMIT Project) and by CPAN, CSPD-2007-00042@Ingenio2010. Calculations were performed in the “Clúster de Cálculo de Alta Capacidad para Técnicas Físicas” funded in part by UCM and in part by UE under FEDER program. This is a contribution to the International Excellence Campus of Moncloa. We would like to acknowledge the support of Matthias Benker from Carl Zeiss Meditec for providing the experimental data as well as Sven Clausen and Frank Schneider for their hospitality and help during the stay of P. Ibáñez at Universitätsklinikum Mannheim.

References:

- Avanzo M, Rink A, Dassie A, Massarut S, Roncadin M, Borsatti E and Capra E 2012 In vivo dosimetry with radiochromic films in low-voltage intraoperative radiotherapy of the breast. *Med Phys*, **39**(5), 2359-68.
- Baro J, Sempau J, Fernández-Varea J M and Salvat F 1995 PENELOPE - an algorithm for Monte Carlo simulation of the penetration and energy-loss of electrons and positrons in matter *Nucl. Instrum. Meth. B*. **100**(1) 31-46.
- Beatty J, Biggs P, Gall K, Okunieff P, Pardo F, Harte K, Dalterio M and Sliski A 1996 A new miniature x-ray device for interstitial radiosurgery: Dosimetry *Med. Phys.* **23**(1):53-62.
- Bouزيد D, Bert J, Dupre P F, Benhalouche S, Pradier O, Bousson N and Visvikis D 2015 Monte-Carlo dosimetry for intraoperative radiotherapy using a low energy x-ray source. *Acta Oncol* **54**(10) 1788-95.
- Brown T A, Hogstrom K R, Alvarez D, Matthews K L II, Ham K and Dugas J P 2012 Dose response curve of EBT, EBT2 and EBT3 radiochromic films to synchrotron-produced monochromatic x-ray beams *Med Phys* **39**(12) 7412-7.
- Capote R, Jeraj R, Ma C, Rogers D, Sanchez-Doblado F, Sempau J, Seuntjens J and Siebers J 2006 Phase-space database for external beam radiotherapy. *Summary report of a consultants' Meeting Technical Report INDC(NDS)-0484*. Vienna, Austria, International Nuclear Data Committee, IAEA.
- Chetty I J, Curran B, Cygler J E, DeMarco J J, Ezzel G, Faddegon B A, Kawrakow I, Keall P J, Liu H and Ma C 2007 Report of the AAPM Task Group No. 105: Issues associated with clinical implementation of Monte Carlo-based photon and electron external beam treatment planning. *Med. Phys.* **34**(12) 4818-53.
- Chiavassa S, Buge F, Hervé C, Delpón G, Rigaud J, Lisbona A and Supiot 2015 Monte Carlo evaluation of the effect of inhomogeneities on dose calculation for low energy photons intra-operative radiation therapy in pelvic area *Phys. Medica* **31** 956-62.
- Chica U, Anguiano M, and Lallena A M 2009 Benchmark of PENELOPE for low and medium energy X-rays. *Phys. Medica*, **25**(2), 51-57.
- Clausen S, Schneider F, Jahnke L, Fleckenstein J, Hesser J, Glatting G and Wenz F 2012 A Monte Carlo based source model for dose calculation of endovaginal TARGIT brachytherapy with INTRABEAM® and a cylindrical applicator *Z. Med. Phys.* **22**(3) 197-204.
- Dinsmore M, Harte K J, Sliski A P, Smith D O, Nomikos P M, Dalterio M J, Boom A J, Leonard W F, Oettinger P E and Yanch J C 1996 A new miniature x-ray source for interstitial radiosurgery: Device Description *Med. Phys.* **23**(1) 45-52.

- 1
2
3
4 Douglas R M, Beatty J, Gall K, Valenzuela R F, Biggs P, Okunieff P and Pardo F S 1996 Dosimetric results from a
5 feasibility study of a novel radiosurgical source for irradiation of intracranial metastases *Int. J. Radiat. Oncol.*
6 **36**(2) 443-50.
- 7 Eaton D and Duck S 2010 Dosimetry measurements with an intra-operative x-ray device. *Phys. Med. Biol.* **55**(12):359.
- 8 Eaton D 2012 Quality assurance and independent dosimetry for an intraoperative x-ray device *Med. Phys.* **39**(11) 6908-20.
- 9 Ebert M A and Carruthers B 2003 Dosimetric characteristics of a low-kV intra-operative x-ray source: implications for
10 use in a clinical trial for treatment of low-risk breast cancer *Med. Phys.* **30**(9) 2424-31.
- 11 Ebert M A, Asad A H, Salim A, Siddiqui S A 2009. Suitability of radiochromic films for dosimetry of low energy X-rays.
12 *J. Appl. Clin. Med. Phys.* **10**(4) 232-40.
- 13 Fernandez-Ramirez C, De Guerra E M, Udías A and Udías J M 2008 Properties of nucleon resonances by means of a
14 genetic algorithm *Phys. Rev. C* **77**(6) 065212.
- 15 Giordano F, Abo-Madyan Y, Brehmer S, Herskind C, Sperk E, Schneider F, Clausen S, Welzel G, Schmiedek P and Wenz
16 F 2014 Intraoperative radiotherapy (IORT) – a resurrected option for treating glioblastoma? *Transl. Cancer Res.*
17 **3**(1) 94-105.
- 18 Guerra P, Udías J M, Herranz E, Santos-Miranda J A, Herraiz J L, Valdivieso M F, Rodríguez R, Calama J A, Pascau J
19 and Calvo F 2014 Feasibility assessment of the interactive use of a Monte Carlo algorithm in treatment planning
20 for intraoperative electron radiation therapy *Phys. Med. Biol.* **59**(23) 7159-79.
- 21 Hensley F W 2017 Present state and issues in IORT *Radiat. Oncol.* **12**(1):37.
- 22 Herranz E, Herraiz J L, Ibáñez P, Perez-Liva M, Puebla R, Cal-González J, Guerra P, Rodríguez R, Illana C and Udías, J
23 M 2015 Phase space determination from measured dose data for intraoperative electron radiation therapy *Phys.*
24 *Med. Biol.* **60**(1) 375-401.
- 25 Hill R, Healy B, Holloway L, Kuncic Z, Thwaites D, and Baldock C 2014 Advances in kilovoltage x-ray beam dosimetry.
26 *Phys. Med. Biol.*, **59**(6), R183.
- 27 Iaccarino G, Strigari L, D'Andrea M, Bellesi L, Felici G, Ciccotelli A, Benassi M and Soriani A 2011 Monte Carlo
28 simulation of electron beams generated by a 12 MeV dedicated mobile IORT accelerator *Phys. Med. Biol.*
29 **56**(14):4579.
- 30 Ibáñez P. 2017a Implementation and validation of ultra-fast dosimetric tools for IORT *PhD Thesis, University*
31 *Complutense of Madrid.*
- 32 Ibáñez P, Villa-Abanza A, Hinault P, Pérez N and Udías J M 2017b Hybrid Monte Carlo for low-energy X-rays intra-
33 operative radiation therapy dose calculation *Physica Medica* **42**: 17.
- 34 Kramers H A 1923 XCIII. On the theory of X-ray absorption and of the continuous X-ray spectrum *Philosophical*
35 *Magazine Series 6* **46**(275) 836-71.
- 36 Kraus-Tiefenbacher U, Scheda A, Steil V, Hermann B, Kehrer T, Bauer L, Melchert F and Wenz F 2005 Intraoperative
37 radiotherapy (IORT) for breast cancer using the INTRABEAM® system *Tumori* **91**(4) 339-45.
- 38 Low D A, Harms W B, Mutic S and Purdy J A 1998 A technique for the quantitative evaluation of dose distributions *Med.*
39 *Phys.* **25**(5), 656-61.
- 40 Ma C M and Jiang S B 1999 Monte Carlo modeling of electron beams from medical accelerators. *Phys. Med. Biol.* **44**(12),
41 157.
- 42 Mücke A, Lewis D F and Yu X 2011 Multichannel film dosimetry with nonuniformity correction. *Med. Phys* **38**(5), 2523-
43 34.
- 44 Nwankwo O, Clausen S, Schneider F and Wenz F 2013 A virtual source model of a kilo-voltage radiotherapy device
45 *Phys. Med. Biol.* **58**(7): 2363-75.
- 46 Pascau J, Santos-Miranda J A, Calvo F A, Bouché A, Morillo V, González-San Segundo C, Ferrer C, López-Tarjuelo and
47 Desco M 2012 An innovative tool for intraoperative electron beam radiotherapy simulation and planning:
48 description and initial evaluation by radiation oncologists. *Int. J. Radiat. Oncol.* **83**(2) 287-95.
- 49 Salvat F, Fernández-Varea J M and Sempau J 2008 PENELOPE- A code system for Monte Carlo simulation of electron
50 and photon transport (Issy-les-Moulineaux: OECD Nuclear Energy Agency)
- 51 Schach von Wittenau A E, Cox L J, Bergstrom P M, Chandler W P, Siantar C L and Mohan R 1999 Correlated histogram
52 representation of Monte Carlo derived medical accelerator photon-output phase space *Med. Phys.* **26**(7) 1196-
53 211.
- 54 Schneider F, Fuchs H, Lorenz F, Steil V, Ziglio F, Kraus-Tiefenbacher U, Lohr F and Wenz F 2009 A novel device for
55 intravaginal electronic brachytherapy *Int. J. Radiat. Oncol.* **74**(4) 1298-305.
- 56 Schneider F, Greineck F, Clausen S, Mai S, Obertacke U, Reis T and Wenz F 2011 Development of a novel method for
57 intraoperative radiotherapy during kyphoplasty for spinal metastases (Kypho-IORT) *Int. J. Radiat. Oncol.* **81**(4)
58 1114-9.
- 59 Schneider F, Bludau F, Clausen S, Fleckenstein J, Obertacke U and Wenz F 2017 Precision IORT- Image guided
60 intraoperative radiation therapy (igIORT) using online treatment planning including tissue heterogeneity
correction *Phys. Medica* **37** 82-7.
- Schneider T, Rouija M and Selbach H J 2010 Absolute Dosimetry for Brachytherapy with the INTRABEAM® miniature
x-ray devices *Radiother. Oncol.* **96** 573
- Sedlmayer F, Reitsamer R, Wenz F, Sperk E, Fussl C, Kaiser J, Ziegler I, Zehentmayr F, Deutschmann H, Kopp P and
Fastner G 2017 Intraoperative radiotherapy (IORT) as boost in breast cancer *Radiat. Oncol.* **12**(1) 23.
- Sempau J, Fernández-Varea J M, Acosta E, and Salvat F 2003 Experimental benchmarks of the Monte Carlo code
PENELOPE. *Nucl. Instrum. Meth. B.* **207**(2) 107-23.
- Sempau, J, Badal A and Brualla J 2011 A PENELOPE-based system for the automated Monte Carlo simulation of clinacs
and voxelized geometries-application to far-from-axis fields *Med. Phys.* **38**(11) 5887-95.

- 1
2
3
4 Sethi A, Emami B, Small W and Thomas T O 2018 Intraoperative radiotherapy with INTRABEAM®: Technical and
5 dosimetric considerations *Front. Oncol.* **8**: 74.
- 6 Sorriaux, J, Kacperek A, Rossomme S, Lee J A, Bertrand D, Vynckier S and Sterpin E 2013 Evaluation of Gafchromic®
7 EBT3 films characteristics in therapy photon, electron and proton beams *Phys. Medica* **29**(6) 599-606.
- 8 Sperk E, Welzel G, Keller A, Kraus-Tiefenbacher U, Gerhardt A, Sütterlin M, and Wenz F 2012 Late radiation toxicity
9 after intraoperative radiotherapy (IORT) for breast cancer: results from the randomized phase III trial TARGIT
10 *A Breast Cancer Res. Tr.* **135**(1) 253-60.
- 11 Steenbeke F, Gevaert T, Tournel K, Engels B, Verellen D, Storme G and De Ridder M 2016 Quality assurance of a 50-kV
12 radiotherapy unit using EBT3 GafChromic film: A feasibility study *Technol. Cancer Res Treat* **15**(1) 163-70.
- 13 Sutherland J G and Rogers D W 2010 Monte Carlo calculated absorbed-dose energy dependence of EBT and EBT2 film
14 *Med Phys* **37**(3) 1110-6.
- 15 Vaidya, J S, *et al.* 2010 Targeted intraoperative radiotherapy versus whole breast radiotherapy for breast cancer
16 (TARGIT-A trial): an international, prospective, randomised, non-inferiority phase 3 trial *Lancet* **376**(9735) 91-
17 102.
- 18 Vaidya, J S, *et al.* 2014 Risk-adapted targeted intraoperative radiotherapy versus whole-breast radiotherapy for breast
19 cancer: 5-year results for local control and overall survival from the TARGIT-A randomised trial *Lancet*
20 **383**(9917) 603-13.
- 21 Valdivieso-Casique M F *et al.* 2015 RADIANCE - A planning software for intra-operative radiation therapy *Transl.*
22 Vidal M, Ibáñez P, Cal-González J, Guerra P and Udías J M 2014a Hybrid Monte Carlo dose algorithm for low energy X-
23 rays intraoperative radiation therapy *Radiother. Oncol.* **111**(1) 117-18.
- 24 Vidal M, Ibáñez P, Guerra P, Herranz E and Udías J M 2014b Realistic on-the-fly dose calculation for low energy X-rays
25 Intra-Operative Radiation Therapy *Radiother. Oncol.* **110** 103-4.
- 26 Wenz F, Schneider F, Neumaier C, Kraus-Tiefenbacher U, Reis T, Schmidt R and Obertacke U 2010 Kypho-IORT-a
27 novel approach of intraoperative radiotherapy during kyphoplasty for vertebral metastases *Radiat Oncol* **5**(1) 11.
- 28 Yanch J C and Harte K J 1996 Monte Carlo simulation of a miniature, radiosurgery x-ray tube using the ITS 3.0 coupled
29 electron-photon transport code *Med. Phys.* **23**(9) 1551-58.
- 30 Ye S J, Brezovich I A, Pareek P and Naqvi S A 2004 Benchmark of PENELOPE code for low-energy photon transport:
31 dose comparisons with MCNP4 and EGS4 *Phys Med Biol* **49**(3) 387-97.
- 32
33
34
35
36
37
38
39
40
41
42
43
44
45
46
47
48
49
50
51
52
53
54
55
56
57
58
59
60